



Research Note

The construction and application of a simplified pore network model based on computerized tomography

Y.T. Xie^{a,*}, Z.H. Chen^b and Z.M. Du^b

a. *State Key Lab of Oil and Gas Reservoir Geology and Exploitation, Southwest Petroleum University, Chengdu, China.*

b. *School of Oil & Natural Gas Engineering, Southwest Petroleum University, Chengdu, China.*

Received 11 April 2015; received in revised form 1 October 2015; accepted 2 February 2016

KEYWORDS

Pore network model;
Flow capacity;
Non-linear flow;
Computerized
tomography.

Abstract. A simplified pore network model, which divided pore structure into cube lattices, was developed based on the digital core extracted from micro computerized tomography (μ -CT) in this study. It rolled the complex topology and connectivity of pore structure into adjacent cubes. The static property of each cube was determined by the statistic CT data. The connectivity of adjacent cubes and flow regime were determined by the capillary pressure difference which is a function of tunnel size, interfacial tension, wet contact angle, and external pressure gradient. In this simplified pore network model, the flow capacity properties are determined by number and size distribution, mobile tunnels, and fluid viscosity. The flow velocity and sweep efficiency are non-linear as mobile tunnels increase nonlinearly with increasing driving force before all tunnels start flowing. The critical pressure gradient that changed the non-linear flow to linear flow was performed as the threshold pressure gradient. The dynamic mobile performance of Oil In Place (OIP) is determined by the number of mobile tunnels and their diameter distribution for different pressure gradients. The relationship of microscopic sweep efficiency, water cut, and pressure gradient to oil recovery can be quantified by flow simulation in this pore network model.

© 2016 Sharif University of Technology. All rights reserved.

1. Introduction

The formation flow capacity is a crucial factor in well productivity and ultimate oil field development efficiency from a theoretical seepage perspective [1]. Flow capacity depends on the rock permeability and fluid viscosity. Small core samples are usually drilled from a full diameter core obtained from the target payzone in the reservoir. The samples are used in laboratory experiments after a series of procedures such as washing, drying, and saturating. The in-situ absolute permeability under different overburden pressures and the relative permeability performance

under different phase saturations are measured in core flooding experiments via changes in temperature, pressure, and fluid saturation. These evaluation methods may not be suitable for heavy oil reservoir [2]. Most of the formation in heavy oil reservoirs is weakly consolidated and may even be unconsolidated. It is difficult to obtain a standard complete cylindrical core from the target layer using the routine coring barrel. In the small core drilling process, the rock skeleton structure suffers structure damage due to the vibration in the sample drilling process. Liquid nitrogen is typically used to freeze loose rock, but the volume expansion of the ice formed from the connate water can change the micro-structure in porous media. During the core washing, drying, and fluid saturation processes, the lead sheath or heat shrinkable sleeve used to maintain the loose core integrity cannot guarantee

*. *Corresponding author. Tel.: +86 13438353246;
Fax: +86 028 83033316
E-mail address: 250268368@qq.com (Y.T. Xie)*

that the inner structure remains intact [3–5]. For core analysis experiments, a confining pressure, 1–1.5 MPa, greater than the inflow pressure is needed to maintain seal in core surface and inner wall of core tank [6]. The radial deformation, caused by sealing procedure, in combination with the internal rock skeleton structure damage, caused by fluid displacement, leads to erroneous analysis of experimental results.

Meanwhile, the development of computational methods to analyze the 3-dimensional (3D) structure of pore networks has made significant advances with the advent of X-ray micro computerized tomography (μ -CT) which allows for the visualization of the internal structure of a rock sample at the micron scale [7–11]. There are no obstacles to obtaining high quality images of the spatial microscopic structure of unconsolidated rock samples without causing any damage [12]. Petrophysical properties such as sound speed, electrical properties, nuclear magnetic resonance response, and flow characteristics that are usually derived from laboratory experiments can now be simulated using CT images [13–14].

Pore scale modelling is another method to describe internal rock structure and study multiphase flow and transport in porous media. It was first introduced by Fatt in the 1950s in his tubes network model [15]. To simplify operations, he replaced the three-dimensional network by a two-dimensional network. Within that model, he calculated the capillary pressure curve and obtained pore size distribution. Since then, many scholars have put lots of efforts on the construction and application of pore network model. Percolation theory was used to describe multiphase flow properties [16–17]. Micro model experiments were used for parameters adjustment. Permeability, wettability, interfacial area, dissolution rate, relative permeability, mass transfer coefficient, and many other physical properties have been predicted [18–25]. Geometry, spatial correlation, and other topological characteristics have been discussed in description of the pore space. Matching geometric parameters with available experiments to build a regular network model or directly modeling the random topology of the pore space were two mainstreams in 1990s [26–28]. Both of them faced limitation; regular network model is limited in prediction because the coordination of data with experiments is non-unique and essential features of the pore space are missing; while, random network models would have similar flow properties if the grain size distributions inferred from thin section analysis were similar to each other [29].

Reconstruction of pore network from μ -CT-scanning images has been studied [30–34]. Computational Fluid Dynamics (CFD) method was the direct method in pore-scale modeling to simulate the

fluid flow by solving the Navier-Stokes equations in 2000s [35]. The dimensions of CT images were more than $1000 \times 1000 \times 1000$ voxels. A pore network based on these images, without simplification, represents a large data set which requires a large amount of memory in CFD application [36]. Due to irregular fluid-solid boundaries and the deformability of fluid-fluid interfaces, direct models are computationally expensive and may not be suitable for studying fluid flow [37]. With the introduction of more sophisticated seepage theories in conventional reservoirs and more unconventional reservoirs being developed, non-linear flow phenomena and their governing mechanisms are receiving increased attention. The pore network modeling technology based on μ -CT image post-processing has gradually become one of the main technologies and methods used in the oil industry [38]. Reconstructing the pore structure from μ -CT scan images more accurately, modeling the pore network more reasonably, and simulating the fluid flow of the pore network more efficiently continue to be the main objectives in this field.

This study aimed at developing a pore network that characterized reservoir rocks more efficiently and simulated the fluid flow process dominated by the combined effects of capillary pressure, viscous forces, and driving pressure within the pore networks. High resolution CT scan was conducted on the core samples obtained from the target layer. The pore spatial location and the pore structure parameters were extracted. Connectivity of each pair of adjacent cubes was investigated under certain condition. A Cartesian coordinate overlapped the sample unit and it was divided into $1000 \times 1000 \times 1000$ blocks. The porosity of each block was calculated from the size and location of each pore. Oil and water two-phase hydrodynamic balance was checked in each connected tunnel to determine the flow ability. The multi-pipe Poiseuille's law and Darcy's equation were applied to calculate the effective permeability that indicated the flow capacity of this scan rock sample. The dynamic effective flow parameters and the non-linear flow mechanism were studied through applying the above procedures in different external pressure gradients and different oil and water saturations. The methodology may then be applied to oil development processes such as studying the flow properties and non-linear flow mechanisms for different external pressure gradients and different water saturations. This will help to validate the 3D description of irreducible oil and to predict the changes in the recoverable reserves.

2. Procedures of modelling

2.1. Obtaining the digital core

Data applied in this pore network model was originally based on μ -CT scan of actual rock samples from Bohai

Bay with a resolution of approximately $10\ \mu\text{m}$. Different mineral types and subject thicknesses in rock were reflected by the X-ray in variable energy attenuation. The intensity of X-ray was measured after it penetrated the rock sample and then the absorption coefficient was calculated. The two-dimensional (2D) micro-structure of matrix and pores in a rock slice was extracted from 2D images and then the 3D micro-structure was reconstructed by image processing algorithms of the projection slices in the same direction. Each 3D pore was described by the maximum ball method. Then, the size and spatial location of each pore were compiled into data sets. The data sets associated with the microscopic pore structure in the rock sample are the so-called digital core.

2.2. Model description

2.2.1. Model construction

The rock model was constructed by stacked particles with different sizes, shapes, and contact relationships. The diameters and connectivity of the inside tunnel network were variously dependent on particle sizes. The status of both flow regime and flow rate depends on the balance between capillary pressure difference which is a function of tunnel size, interfacial tension, wet contact angle, and external pressure gradient.

2.2.2. Model assumptions

- There was no absolutely dead end tunnel in the rock;
- The size and connectivity of a tunnel depended on particle size;
- There was no rock deformation during the production period;
- The surface of rock tunnels was completely water wet;
- All tunnels were initially saturated with water;
- The inside tunnel network was saturated with water and oil;
- The flow was assumed to be laminar.

2.2.3. Flow process

The external pressure gradient arises either from buoyancy due to the density difference between oil and water or from the pressure drawdown of production well. If the external pressure gradient is higher than the threshold pressure in the largest tunnel in the pore network, the fluid initially starts flowing through that tunnel. With increase in driving pressure, fluid starts flowing in the smaller tunnel. As a result, the volumetric sweep efficiency in the pore network increases and the flow capacity of rock is enhanced. Therefore, the apparent flow velocity, which is the function of flow section area, is non-linear since the flow section area increases as more tunnels are involved.

2.2.4. Saturation history

During the hydrocarbon accumulation period, some tunnels were gradually displaced by the oil with lighter density under the action of buoyancy. Meanwhile, the others were still saturated with water since the buoyancy was less than the threshold pressure. The oil displaced by water in each tunnel obeyed the sequence of resistance from small to large. At the end of water flooding, all pores were saturated with water, completely.

2.3. Construction of digital core

The setting of CT-scanning resolution affects the image clarity and the accuracy of pore structure identification. With higher resolution setting, the intensity and penetrability of X-ray will be higher and stronger. Improper resolution setting may bring in overexposure or underexposure that result in poor imaging of pore structure inside a rock sample. The grain size-distribution of target rock sample ranges from 20 to $300\ \mu\text{m}$, then the scanning resolution should be set at $10\ \mu\text{m}$.

After CT-scanning of the rock sample, a three-dimensional Cartesian coordinate system, corresponding to the in-situ flow direction in the reservoir, is created. The diameter of core plug is 2.5 cm. To exclude the impact of cutting process on inner pore structure, the center of scanning area is placed at the core of the rock sample and the scanning area is set as a cube with 1 cm of length of edge. Based on the $10\ \mu\text{m}$ scanning resolution and 1 cm length of the scanning area, the digital core unit is divided into $1000 \times 1000 \times 1000$ blocks. The edge length of each cube is $10\ \mu\text{m}$ (Figure 1).

The porosity of the digital core is defined as the ratio of identified pore volume to the total volume of scanning area. The porosity of each block is based on the size and location of each recognized pore in the digital core (Figure 2). Equivalent sphere should be used to identify the radius and location of each pore from each 2D scanning image. Eq. (1) is applied to calculate porosity of the 3D digital core. The threshold of pore color is determined by the digital core porosity fitted with rock porosity from experiment.

The connectivity between blocks $i - 1$ and $i + 1$ is

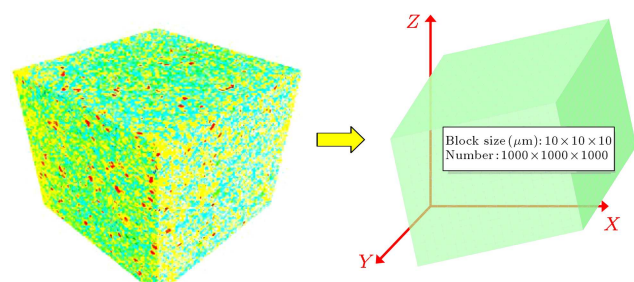


Figure 1. Block system of the digital core.

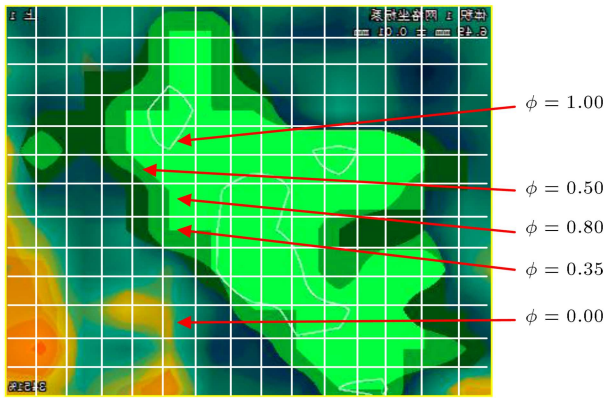


Figure 2. Porosity in the blocks.

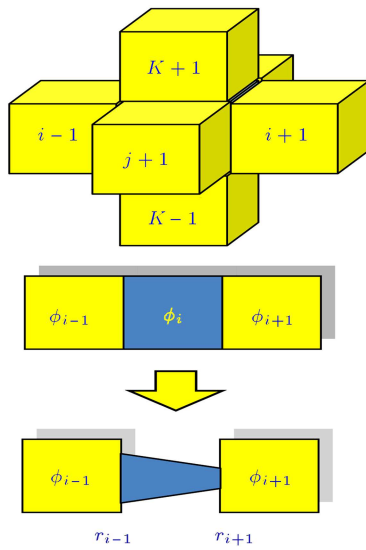


Figure 3. Connection between blocks.

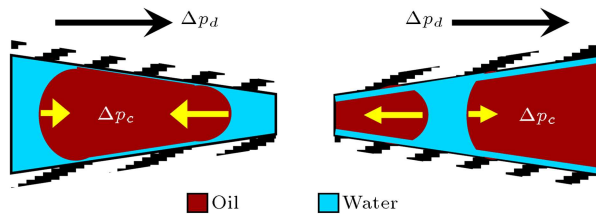


Figure 4. Flow status in a tunnel of varying diameters.

determined by the radius of a cylinder whose volume is equal to block i (Figure 3). If the porosity of block i is greater than 0, blocks $i-1$ and $i+1$ will be connected. If the porosity of block $i-1$ is equal to the porosity of block $i+1$, the radius of the cylinder-connected blocks $i-1$ and $i+1$ will be the same at each end, which means there is no flow resistance between blocks $i-1$ and $i+1$.

Otherwise, the radius of the cylinder-connected blocks $i-1$ and $i+1$ will be different at each end. The flow resistance can be calculated by Eq. (5). The capillary pressure difference is the resistance in a water wet tunnel of varying sizes (Figure 4). Only when the

driving pressure gradient overcomes the flow resistance will the fluid start flowing.

2.4. Flow parameters calculation

Based on the geometry of each tunnel in the block system of the digital core, the porosity of the pore network unit is defined as:

$$\phi = \frac{\sum_{i=1}^n \pi r_i^2 \tau_i \Delta L}{\Delta L} = \sum_{i=1}^n \pi r_i^2 \tau_i. \quad (1)$$

The total flow rate of all tunnels in cross-section is expressed, using Poiseuille's law, as:

$$q = \frac{\pi}{8\mu} \sum_{i=1}^n \left(\frac{ar^4}{\tau} \right)_i \frac{\Delta P}{\Delta L}. \quad (2)$$

Substituting Eq. (2) into Darcy's equation, the permeability of the pore network unit can be expressed as:

$$K = \frac{q}{A} \frac{\mu \Delta L}{\Delta P} = \frac{\frac{\pi}{8\mu} \sum_{i=1}^n \left(\frac{ar^4}{\tau} \right)_i \frac{\Delta P}{\Delta L} \mu \Delta L}{A \Delta P} = \frac{\pi}{8} \sum_{i=1}^n \frac{r_i^4}{\tau_i}. \quad (3)$$

The relationship between porosity and permeability is given as:

$$K = \frac{\varphi}{8} \sum_{i=1}^n \left(\frac{r}{\tau} \right)_i^2. \quad (4)$$

The capillary pressure between each pair of connected blocks is given as:

$$\Delta P_c = 2\sigma_{ow} \cos \theta_{ow} \left(\frac{1}{r_1} - \frac{1}{r_2} \right). \quad (5)$$

2.5. Flow capacity evaluation

For the underground reservoir, the pressure gradient increases gradually from 0 to a steady value with the increased well production. For pore network model, the capillary pressure was calculated by Eq. (5) for each pair of connected blocks in ascending order. The blocks that have a capillary pressure lower than the driving pressure but have not been displaced are identified. The driving pressure increases and the searching process is repeated until no more blocks can be displaced. This is the process of pressure propagation in the pore network model.

The curve for the number of mobile tunnels can be obtained using the number of all the involved blocks for different driving pressures.

The effective permeability of each phase is calculated by Eq. (3) based on the size of all mobile tunnels saturated with the given phase. Based on

microscopic oil-water two phase displacement process, sweep efficiency under different pressure gradients and effective permeability at variable water saturation can be determined.

Applying Eq. (2) can get the flow velocity in pore network model. The flow velocity in one pore network unit is converted to apparent flow velocity in a rock sample (dividing flow velocity by cross-sectional area) for analysis of the relationship between the apparent flow velocity and the external pressure gradient. The relation of flow velocity to pressure gradient is nonlinear before all the tunnels start flowing. The threshold pressure gradient and the initial pressure gradient of the linear flow were determined when all the tunnels in the pore network were mobile.

The pore volume percentage in the mobile area and its contribution to oil recovery were calculated for different driving pressures. The additional driving pressure gradient required to increase the recovery factor was predicted based on the amount of reserves available at each pressure gradient level. Water flooding process in pore network model was simulated by increasing driving pressure. The simulated results of how oil recovery changed with water cut increase can be used to evaluate the EOR potential. Based on parallel-pipe flow principle – the flow velocity in the pipe is proportional to the square of pipe diameter – the elapsed time to reach a given recovery factor corresponding to a particular pressure gradient can be calculated.

3. Case study and discussion

3.1. Geometric characteristics

The data of digital core based on CT-scanning of target layer rock sample shows that there is a reciprocal relationship between number of tunnels and tunnel diameter (Figure 5). The relationship between the pore

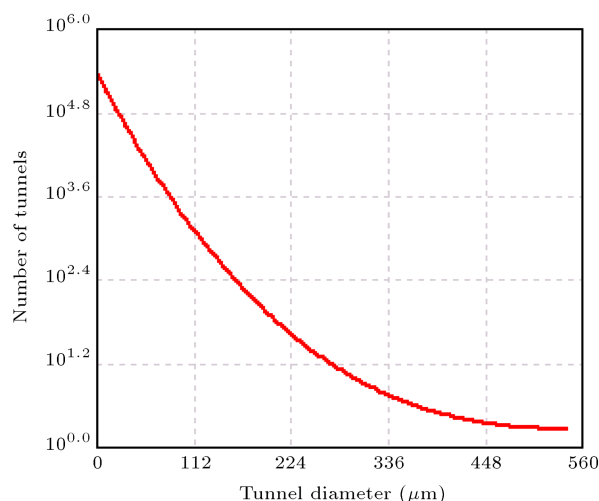


Figure 5. Tunnel diameter distribution.

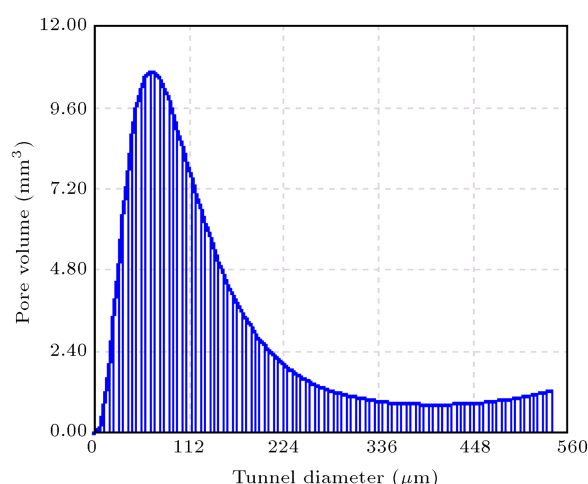


Figure 6. Distribution of tunnel volume.

volume and tunnel diameter resembles a skewed normal distribution (Figure 6), which agrees with core lab experiments. Many core particle size tests show that the size of mineral particles in rock sample is roughly normally distributed and the number of particles is exponentially distributed.

Controlled by lithology of parent rocks, deposition and diagenesis, reservoir formation is heterogeneous and anisotropic. The size, space form, and connectivity of pores in porous media are complex to describe mathematically. Applying statistics from digital core can be used as an alternative method. The statistics of digital core show that there are more small pores than large ones in the rock, but the total volume is smaller. Medium size pores own the largest number and occupy most of the volume of the rock sample. All these characteristics will affect the storage and flow capacity of a reservoir.

3.2. Flow properties and flow regime

Based on the method described in Section 2 and the statistics of digital core from CT-scanning, the pore network model of rock sample has been built using the percolation theory described in Section 2 to calculate the flow capacity and simulate the flow process in the pore network model. The pore network simulation shows that the number of mobile tunnels and the microscopic sweep efficiency start at zero and increase with higher driving pressure gradients (Figures 7 and 8). Tunnels with larger diameter turn to mobile more easily than smaller ones that have a higher resistance. As a result, the flow is non linear in porous media like rocks that are characterized by variable pore size and connectivity. Figure 9 shows that the permeability gradually increases with increase in the pressure gradient. It plateaus at the absolute permeability if no more tunnels can become mobile and contribute to the flow capacity in the porous network as the driving pressure increases. Figure 10 shows

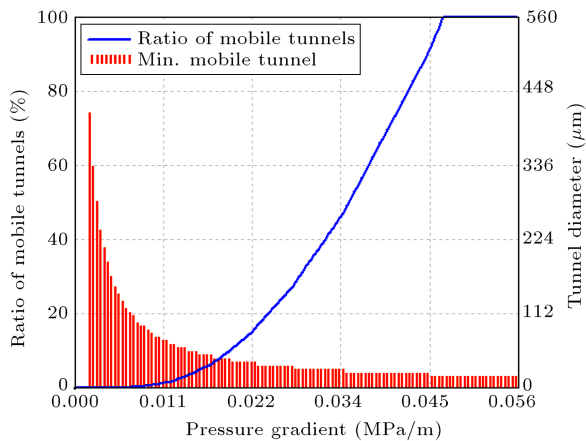


Figure 7. Ratio of mobile tunnels.

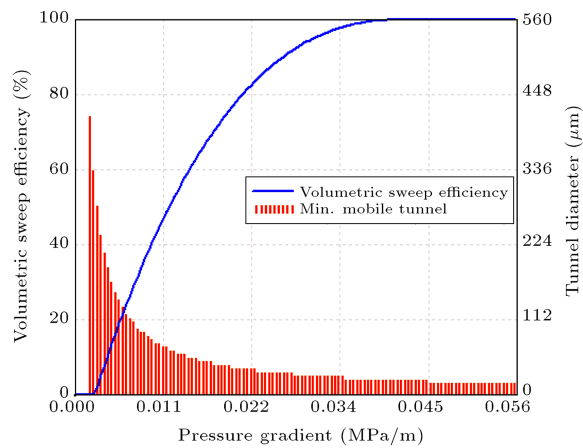


Figure 8. Volumetric sweep efficiency.

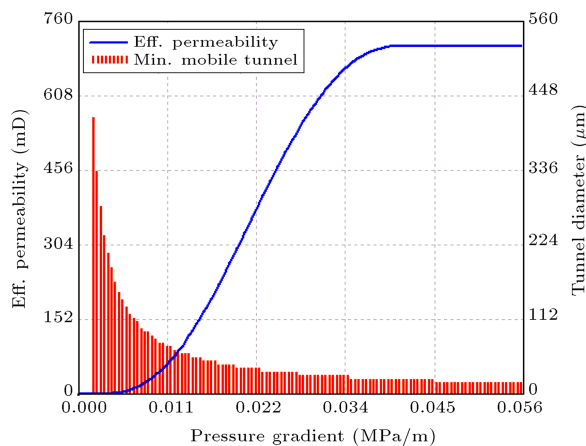


Figure 9. Effective permeability.

that the apparent flow velocity changes from standstill through a non-linear regime to a linear flow regime as the driving pressure gradient is increased.

3.3. Recoverable reserves during pressure depletion

The in-situ pressure continuously decreases with the pressure decrease propagating from the drawdown

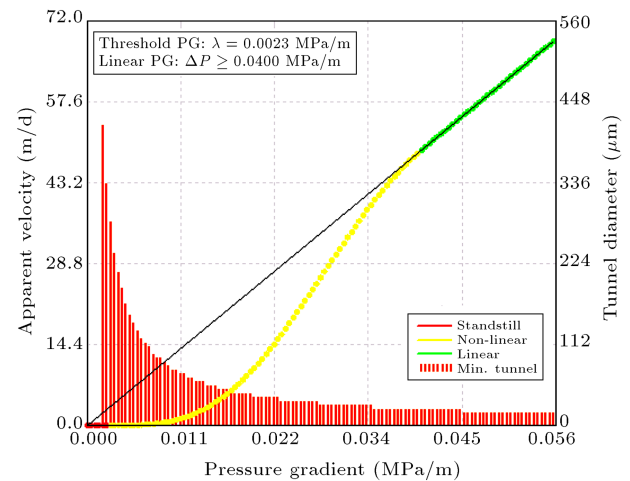


Figure 10. Non-linear flow mechanism.

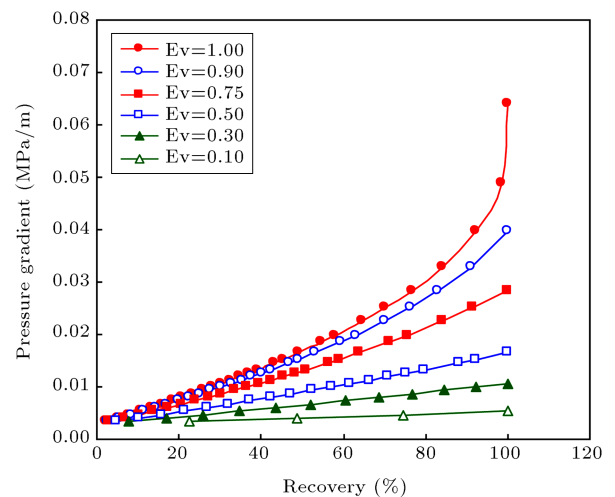


Figure 11. Maximum driven pressure gradient.

point to the remaining portions of the reservoir. From a microscopic point of view, large tunnels become mobile first followed by smaller tunnels. At any moment, the recoverable reserve is the total amount of oil in each mobile tunnel in the pore network. The dynamic mobile performance of Oil In Place (OIP) was studied based on the number of mobile tunnels and their diameter distribution for different pressure gradients. Figure 11 shows that the pressure gradient required to achieve a given amount of recovery for different microscopic volumetric sweep efficiencies. A lower pressure gradient is required to reach the same recovery for lower sweep efficiencies, since the larger tunnels have a higher oil content and lower resistance to becoming mobile. As shown in Figure 12, a higher microscopic sweep efficiency is achieved if more small tunnels are mobile at higher pressure gradients.

The microscopic mechanism can explain how reservoirs with a higher porosity and permeability can achieve a higher recovery using a lower production drawdown. In addition, the production rate dramati-

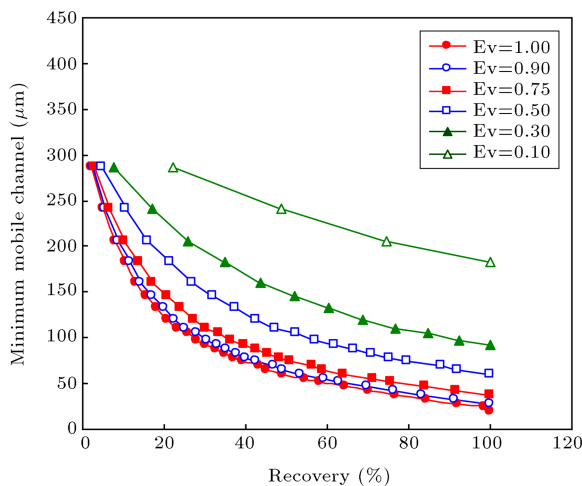


Figure 12. Minimum mobile tunnels.

cally decline in low-mobility reservoirs such as heavy oil and compact reservoirs. This is because the effective in-situ flow capacity in this kind of reservoir is lower than those in the laboratory. As a result, only larger tunnels are mobile for lower sweep efficiencies and mobile area. In this situation, oil recovery can be enhanced using the mobility of smaller tunnels by applying higher pressure gradients through production well infill and an increase in production drawdown.

3.4. Recoverable reserves during water displacement

The saturation and distribution of connate water formed during hydrocarbon accumulation are dependent on the viscosity and density of oil and the diameters of tunnels of the rock. Oil initially saturates tunnels of larger diameter and good connectivity. Therefore, smaller tunnels with poor connectivity are saturated with water. Initial oil migration simulations show that the saturation and distribution of connate water vary based on oil viscosity and pore size (Figure 13).

A higher oil viscosity leads to a higher initial water saturation and a lower initial mobility of oil, as shown in Figure 14. The results of the simulations

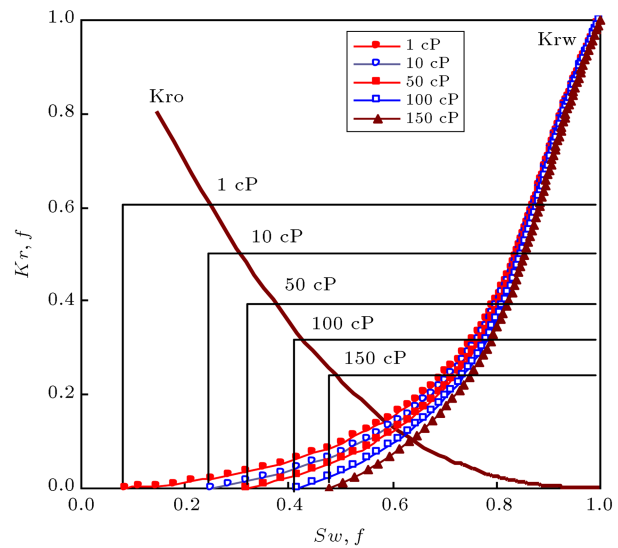


Figure 14. Relative permeability (K_r) at different oil viscosities.

show that oil and water coexist in the heterogeneous reservoir. There is initially connate water in heavy oil reservoir. This means that there is no unified oil and water contact surface and no piston-like displacement even in this microscopic pore network. Connate water will be mobile and will be produced when the pressure gradient is greater than the resistance in the tunnels. This is governed by capillary pressure difference in tunnels with varying diameters. During water flooding, the mobile water will first access the largest tunnel in a pore node with different flow directions and tunnel diameters, then enter the second largest tunnel at a higher pressure gradient. This dynamic process is quantitatively and visually simulated by the current pore network model and the relationship between the water cut and recovery is shown in Figure 15. In the rock model unit, the largest tunnels are first displaced by water until the water cut reaches 0.1 and the oil recovery is 0.19 which corresponds to the oil content in the tunnels. As the pressure gradient increases, the oil in smaller mobile tunnels is displaced by water and more oil is produced by water flooding, as shown in

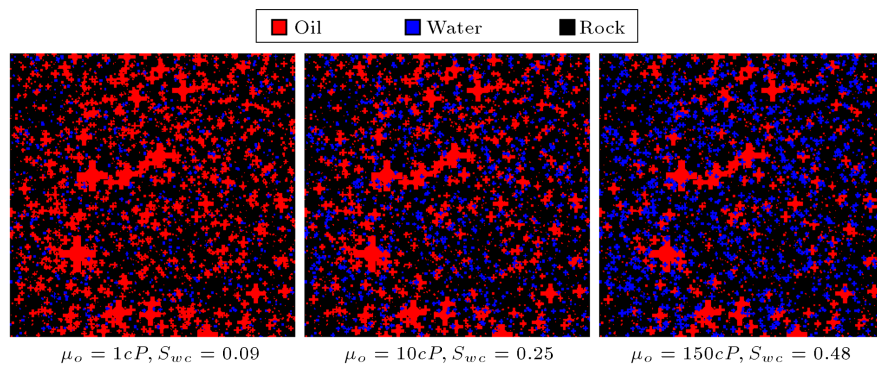


Figure 13. Connate oil and water distribution for different oil viscosities.

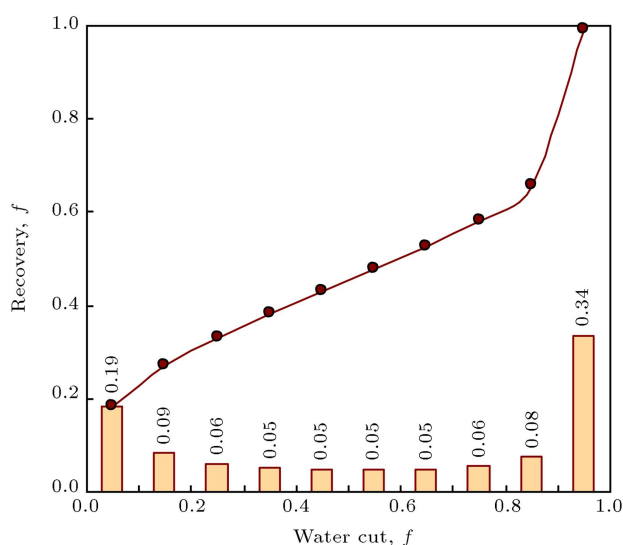


Figure 15. Period of recovery, decimal, during water cut.

Figure 15. The water cut increases to 0.2 and the oil recovery increases to 0.28. The relationship between the water cut and oil recovery is non-linear because the size distribution and connectivity in tunnels are non-uniform. The residual oil saturation is 0.34 and the water cut reaches 1.0. Therefore, it can be concluded that the amount of oil stored in the non-mobile smaller tunnels at this pressure gradient is significantly higher than that in larger ones. The oil recovery can be enhanced by increasing the pressure gradient to improve the sweep efficiency.

3.5. Performance of oil recovery

In the current microscopic pore network model, the dimensionless production period is defined as the ratio of the end time of displacement in the smallest tunnel to the end time in the largest tunnel. Compared to a large-scale reservoir, the end time of displacement in the largest tunnel can be regarded as the period of water breakthrough into production well. Hence, the production period to reach a certain recovery can be based on the dimensionless time.

Simulations were performed for three rock samples with average permeability values of 193 mD, 482 mD, and 1066 mD. The results show that the recovery will reach 0.37, 0.40, and 0.45 after 20 production periods and will reach 0.52, 0.57, and 0.63 after 40 production periods. Theoretically, the oil recovery could reach 0.80 in the dimensionless production periods of 83, 102, and 132 for each rock sample, respectively (Figure 16). This shows that a higher recovery can be achieved in a reservoir with higher permeability and over a shorter production time. As development continues, the recovery increment will gradually slow down since the produced oil mainly comes from smaller tunnels with poor connectivity during pressure depletion and water flooding. In the

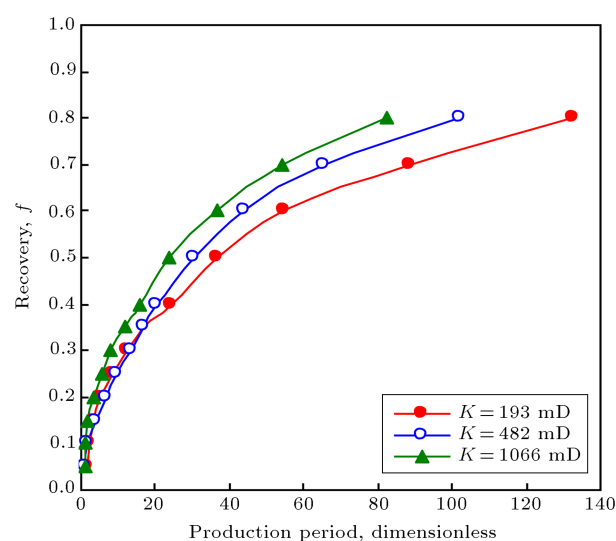


Figure 16. Maximum recovery at different dimensionless production period.

pay layer of the reservoir, it is a reasonable assumption that the in-situ pressure gradient due to production is greater than buoyancy. Therefore, it is theoretically possible to recover 100% of the oil as each tunnel that has been filled with oil can be displaced with water. However, this is not the case in practice, because the development life cycle is limited due to technological constraints, economical factors, the lease period, and other factors. The optimized production rate can be estimated using the proposed methodology based on the development, cost, and profit targets.

4. Conclusions

1. As an alternative of laboratory core experiments, pore network model, based on micro Computerized Tomography (μ -CT), can be used to determine porosity, permeability, and flow capacity properties (relative permeability, flow velocity, sweep efficiency, etc.) of a rock sample;
2. The simplified pore network model was built to characterize the pore structure of reservoir rock and simulate the transport in such porous media, more efficiently. It rolls the complex topology and connectivity of pore structure into adjacent cubes. The static property of each cube is determined by the statistics of CT data. The connectivity and flow regime are determined by the capillary pressure difference of adjacent cubes. The pressure difference is a function of tunnel size, interfacial tension, wet contact angle, and external pressure gradient;
3. In this simplified pore network model, the flow capacity properties are determined by the number and size distribution, mobile tunnels, and fluid viscosity.

The flow velocity and sweep efficiency are non-linear as the mobile tunnels increase nonlinearly with increase in driving force before all tunnels start flowing. The critical pressure gradient that changed the non-linear flow to linear flow was performed as the threshold pressure gradient;

4. The dynamic mobile performance of Oil In Place (OIP) is determined by the number of mobile tunnels and their diameter distribution for different pressure gradients. Higher microscopic sweep efficiency can be achieved as more small tunnels are available at higher pressure gradients;
5. Since oil and water coexist in the heterogeneous reservoir, there is no unified oil and water contact surface and no piston-like displacement even in microscopic pore network. The relationship between the water cut and oil recovery is non-linear because the size distribution and connectivity in tunnels are non-uniform. However, oil recovery is roughly proportional to the pressure gradient increment. It can be quantified by flow simulation in this pore network model. The production period to reach a certain recovery can be based on the dimensionless time;
6. In further studies, specific micrometer-scale core experiments are needed to verify the method. More fitting methods are needed to improve the accuracy of simulation of pore network model.

Acknowledgment

The authors are grateful for the financial support of Open Fund Project (No. CCL2013RCPS0235GNN) provided by the State Key Laboratory of Offshore Oil Exploitation of China.

Nomenclature

A	Cross-sectional area of pore network unit, cm^2
a	Tunnel cross-sectional area, cm^2
K	Permeability, μm^2
N, n	Area density of tunnels, m^{-2}
q	Volumetric flow rate, cm^3/s
r, r_1, r_2	Tunnel radius, cm
S_{wc}	Connate water saturation, %
ΔL	Length of core and length of pore network unit, cm
$\Delta P, \Delta Pd$	Displacement pressure, MPa
ΔPc	Capillary pressure difference, MPa
τ	Tunnel tortuosity, dimensionless
ϕ	Porosity, %

σ_{ow}	Oil-water interfacial tension, N/m
θ_{ow}	Wetting contact angle, angle
μ	Viscosity, mPa.s

References

1. Aghaei, A. and Piri, M. "Direct pore-to-core up-scaling of displacement processes: Dynamic pore network modeling and experimentation", *Journal of Hydrology*, **522**, pp. 488-509 (2015).
2. Kaviani, D. and Jensen, J.L. "Reliable connectivity evaluation in conventional and heavy oil reservoirs: A case study from Senlac heavy oil pool", In *Proceedings of the Canadian Unconventional Resources and International Petroleum Conference*, Alberta, Canada. SPE-137504-MS (2010).
3. Torabi, F., Zarivnyy, O. and Mosavat, N. "Developing new Corey-based water/oil relative permeability correlations for heavy oil systems", In *Proceedings of the SPE Heavy Oil Conference-Canada*, Alberta, Canada. SPE-165445-MS (2013).
4. Mattax, C., McKinley, R. and Clothier, A. "Core analysis of unconsolidated and friable sands", *Journal of Petroleum Technology*, **27**(12), pp. 1423-1432 (1975).
5. Bretz, R.E., Specter, R.M. and Orr Jr, F.M. "Effect of pore structure on miscible displacement in laboratory cores", *SPE Reservoir Engineering*, **3**(03), pp. 857-866 (1988).
6. Musin, K., Khisamov, R. and Dinmuhamedov, R. "Solution to problem of evaluation of unconsolidated heavy oil reservoirs in tatarstan", In *SPE Russian Oil and Gas Conference and Exhibition.*, Society of Petroleum Engineers (2010).
7. Professional committee for standardization of oil and gas field development, *The Oil and Gas Industry Standard of the People's Republic of China-SY/T 5336-1996-Method of Core Routine Analysis*, China national petroleum corporation (1996).
8. Honarpour M.M., Cromwell V., Hatton D., et al. *Reservoir Rock Descriptions Using Computed Tomography (CT)*. In *SPE Annual Technical Conference and Exhibition*, Society of Petroleum Engineers (1985).
9. Pierret, A. and Moran, C. "Quantification of orientation of pore patterns in x-ray images of deformed clay", *Microscopy Microanalysis Microstructures*, **7**, pp. 421-431 (1996).
10. Okabe, H. and Blunt, M.J. "Pore space reconstruction using multiple-point statistics", *Journal of Petroleum Science and Engineering*, **46**, pp. 121-137 (2005).
11. Magaña, B.O., Domínguez, J.D., Ruelas, R., Tarquis, A.M., Gomez-Barba, L. and Andina, D. "Identification of pore spaces in 3D CT soil images using PFCM partitional clustering", *Geoderma*, **217-218**, pp. 90-101 (2012).
12. Likos, W.J. "Quantification of grain, pore, and fluid microstructure of unsaturated sand from x-ray computed tomography images", *Geotechnical Testing Journal*, **35**(6), pp. 911-923 (2012).

13. Elliott, J.C. and Dover, S.D. "X-ray micro-tomography", *Journal of Microscopy*, **126**, pp. 211-213 (1982).
14. Dvorkin, J., Fang, Q. and Derzhi, N. "Etudes in computational rock physics: Alterations and benchmarking", *Geophysics*, **77**(3), pp. D45-D52 (2012).
15. Youssef S., Rosenberg E., Kenter J., et al. "High resolution CT and pore-network models to assess petrophysical properties of homogeneous and heterogeneous carbonates", In *SPE/EAGE Reservoir Characterization and Simulation Conference*, Society of Petroleum Engineers (2007).
16. Fatt, I. "The network model of porous media I. Capillary pressure characteristics", *Trans AIME*, **207**, pp. 144-159 (1956).
17. Koplik, J. "Creeping flow in two-dimensional networks", *Journal of Fluid Mechanics*, **119**, pp. 219-247 (1982).
18. Wilkinson, D. and Willemsen, J.F. "Invasion percolation: A new form of percolation theory", *Journal of Physics A: Mathematical and General*, **16**(14), p. 3365 (1983).
19. Larsen, J.K., Bech, N. and Winter, A. "Three-phase immiscible WAG injection: Micromodel experiments and network models", In *SPE/DOE Improved Oil Recovery Symposium*, Society of Petroleum Engineers (2000).
20. Lenormand, R., Zarcone, C. and Sarr, A. "Mechanisms of the displacement of one fluid by another in a network of capillary ducts", *Journal of Fluid Mechanics*, **135**, pp. 337-353 (1983).
21. Fenwick, D.H. and Blunt, M.J. "Three-dimensional modeling of three phase imbibition and drainage", *Advances in Water Resources*, **21**(2), pp. 121-143 (1998).
22. Thauvin, F. and Mohanty, K.K. "Network modeling of non-Darcy flow through porous media", *Transport in Porous Media*, **31**(1), pp. 19-37 (1998).
23. Blunt, M.J. "Physically-based network modeling of multiphase flow in intermediate-wet porous media", *Journal of Petroleum Science and Engineering*, **20**(3), pp. 117-125 (1998).
24. Fischer, U. and Celia, M.A. "Prediction of relative and absolute permeabilities for gas and water from soil water retention curves using a pore-scale network model", *Water Resources Research*, **35**(4), pp. 1089-1100 (1999).
25. Man, H.N. and Jing, X.D. "Network modelling of wettability and pore geometry effects on electrical resistivity and capillary pressure", *Journal of Petroleum Science and Engineering*, **24**(2), pp. 255-267 (1999).
26. Lerdahl, T.R., Oren, P.E. and Bakke, S. "A predictive network model for three-phase flow in porous media", In *SPE/DOE Improved Oil Recovery Symposium*, Society of Petroleum Engineers (2000).
27. Jerauld, G.R. and Salter, S.J. "The effect of pore-structure on hysteresis in relative permeability and capillary pressure: Pore-level modeling", *Transport in Porous Media*, **5**(2), pp. 103-151 (1990).
28. Bryant, S.L., King, P.R. and Mellor, D.W. "Network model evaluation of permeability and spatial correlation in a real random sphere packing", *Transport in Porous Media*, **11**(1), pp. 53-70 (1993).
29. Hilpert, M. and Miller, C.T. "Pore-morphology-based simulation of drainage in totally wetting porous media", *Advances in Water Resources*, **24**(3), pp. 243-255 (2001).
30. Dong, H. and Blunt, M.J. "Pore-network extraction from micro-computerized-tomography images", *Physical Review E Statistical Nonlinear & Soft Matter Physics*, **80**(2), pp. 1957-1974(2009).
31. Delerue J.F., Perrier E., Yu Z.Y., et al. "New algorithms in 3d image analysis and their application to the measurement of a spatialized pore size distribution in soils", *Physics and Chemistry of the Earth, Part A: Solid Earth and Geodesy*, **24**(99), pp. 639-644 (1999).
32. Zhang X.H, Q. J, X. B. "Comparisons of static, quasi-static and dynamic 3D porous media scale network models for two-phase immiscible flow in porous media", *New Trends in Fluid Mechanics Research*, Springer Berlin Heidelberg, pp. 530-533 (2009).
33. Al-Kharusi, A.S. and Blunt, M.J. "Network extraction from sandstone and carbonate pore space images", *Journal of Petroleum Science and Engineering*, **56**, pp. 219-231 (2007).
34. Raoof, A. and Hassanizadeh, S.M. "A new method for generating pore-network models of porous media", *Transport in Porous Media*, **81**, pp. 391-407 (2010).
35. Jiang, Z., Dijke, M.I.J.V., Wu, K., et al. "Stochastic pore network generation from 3D rock images", *Transport in Porous Media*, **94**(2), pp. 1-23 (2011).
36. Schena G., Favretto S., Piller M., et al. "Pore space characterisation and permeability prediction using fast network extraction and pore throat conductance calculation", In *70th EAGE Conference and Exhibition Incorporating SPE EUROPEC* (2008).
37. Marcke, P.V., Verleye, B., Carmeliet, J., et al. "An improved pore network model for the computation of the saturated permeability of porous rock", *Transport in Porous Media*, **85**, pp. 451-476 (2010).
38. Aghaei, A. and Piri, M. "Direct pore-to-core up-scaling of displacement processes: Dynamic pore network modeling and experimentation", *Journal of Hydrology*, **522**, pp. 488-509 (2015).

Biographies

Yiting Xie was born in 1987. She is a PhD candidate in the Department of Petroleum and Nature Gas Institute at Southwest Petroleum University, Chengdu, China. She has worked as a part-time staff member in

Titan-Petro Ltd. since 2013. She has been studying porous media flow mechanism experiments and mathematic modeling, sand management production control, reservoir numerical simulation, and well production optimization for more than 6 years.

Zhaohui Chen was born in 1970. Dr. Chen is technical director of Titan-Petro Ltd. and a reservoir engineer with more than 20 years of experience in research and oil/gas field development planning and reservoir evaluation. Also, he has assisted clients to make the most profitable reservoir development strategy and worked on underbalanced drilling design, sand management production control, integrated geomechanical reservoir simulation, well production optimization, EOR, and geomechanical laboratory testing.

He has extensive experience in development of loosen sand heavy oil reservoir and loosen sand multi-layer gas reservoirs.

Zhimin Du was born in 1953. She is the Professor of Petroleum and Nature Gas Institute and the former president of Southwest Petroleum University, Chengdu, China. She received her BSc in Oil Production Engineering from Southwest Petroleum Institute in 1978 and was a fellow at Germany's Clausthal Technical University from 1985 to 1988. Her research interests include a broad area of topics in the theories and application of complex oil gas reservoirs development. Recently, she has been focusing on grid simulation and parallel computation of fractured oil reservoir based on unstructured hexahedral